International Journal of Biomedical Data Mining
ISSN: 2090-4924

Rastinehad et al., Biomedical Data Mining 2015, 3:2
DOI: 10.4172/2090-4924.1000106

Case Report Open Access

# Intraductal Carcinoma of the Prostate Diagnosed by Multi-Parametric Prostate Magnetic Resonance Imaging (MRI) and MRI/Ultrasound Fusion-Guided Biopsy

**Ardeshir R Rastinehad[1,3]*, Mathew Fakhoury[1], Simpa S Salami[1], Oksana Yaskiv[2], Omid Rofeim[1], Robert Villani[3], Eran Ben-Levi[3]**

[1]*The Arthur Smith Institute for Urology, Hofstra North Shore-LIJ School of Medicine, New Hyde Park, NY 11042, USA*

[2]*Department of Pathology, Hofstra North Shore-LIJ School of Medicine, New Hyde Park, NY 11042, USA*

[3]*Department of Interventional Radiology, Hofstra North Shore-LIJ School of Medicine, New Hyde Park, NY 11042, USA*

## Abstract

Intraductal carcinoma of the prostate (IDC-P) is an aggressive form of prostate cancer (CaP) with clinical and pathological features distinguishing it from high-grade prostatic intraepithelial neoplasia (HG-PIN). IDC-P is characterized by a high volume and high-grade disease, with an aggressive behavior. We present the case of a 63-year-old male with diagnostic MRI imaging indicative of IDC-P. To our knowledge, this is the first reported case of IDC-P identified with multi-parametric MRI.

**Keywords:** Prostate imaging; Prostate fusion biopsy

## Introduction

Although, the term "intraductal carcinoma of the prostate" (IDC-P) was first used by Rhamy [1], McNeak and Yemoto, were the first to delineate IDC-P as a distinct biological entity with definable histological and clinical features [2]. IDC-P is defined as a proliferation of malignant prostate adenocarcinoma cells distending or completely spanning the lumen of pre-existing prostatic ducts and acini, with at least focal preservation of basal cells. Watts et al. estimated the incidence of IDC-P to 2.8% in prostate biopsies [3].

Histological criteria for the diagnosis of IDC-P include solid; dense cribriform (>50% cellularity of the lumen); trabecular/micropapillary; and loose cribriform intraductal proliferation of malignant cells. The latter two growth patterns share much similarity with HGPIN. In these instances, additional diagnostic criteria, such as marked nuclear pleomorphism (nuclear enlargement > 6x normal nuclei), and non-focal comedonecrosis (> 1 duct showing comedonecrosis) are criteria needed to differentiate it from HGPIN.

The presence of IDC-P in biopsy specimens is regarded as a marker of aggressive disease and definitive therapy is often recommended even in the absence of invasive adenocarcinoma [4-6]. The presence of IDC-P in radical prostatectomy (RP) specimens is often associated with high Gleason Score (Gleason 4 or 5), larger tumor volume, greater probability of extraprostatic extension, positive surgical margin and high biochemical recurrence rate [6,7]. The use of preoperative imaging for diagnosis has never been described. Herein, we report a case of IDC-P diagnosed with multiparametric (MP-MRI) with endorectal coil.

## Case Presentation

A 63-year-old Caucasian male with no significant comorbidities presented with a history of elevated serum PSA levels (4 to 12.17 ng/mL), PSA velocity of 14.51 ng/mL/year; PSA doubling time of 4.51 months; and a total of 5 previous negative prostate biopsies. One previous biopsy showed extensive HG-PIN. Of note, his father was diagnosed with Prostate Cancer (CaP) at age 75, resulting in his death. Digital rectal examination revealed a benign gland.

He underwent MP-MRI of the prostate at an outside institution that demonstrated an intermediate lesion in the left prostatic lobe consistent with HG-PIN or prostatitis; hence no prostate biopsy was done at the time. As shown in Figure 1, MP-MRI (See Appendix A for MRI Parameters) done two years later at our institution showed marked central gland hyperplasia with mass effect on the bladder

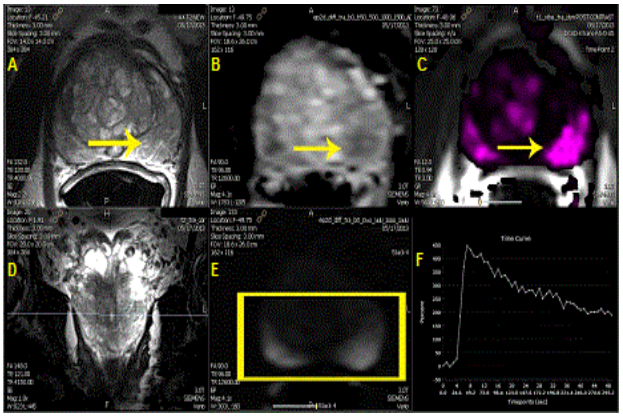


**Figure 1:** 3T Multi-Parametric MRI of the Prostate with an endorectal coil. The largest lesion is denoted by the yellow arrow. A. T2 weighted axial image showing bilateral heterogeneous low signal lesions within the gland. B. ADC map with bilateral restricted areas within the peripheral zone (largest arrow). C. DCE with bilateral enhancement a ktrans map. D. T2 coronal image showing diffuse heterogenous low signal. E. b-2000 DWI image with bilateral high signal throughout the gland. F. DCE contrast enhancement type III curve.

***Corresponding author:** Ardeshir R Rastinehad, D.O, The Arthur Smith Institute for Urology, Hofstra North Shore-LIJ School of Medicine, 450 Lakeville Rd, Suite M-41,New Hyde Park, NY 11040, USA, Tel: 516-734-8500; Fax: 516-734-8537; E-mail: arastine@nshs.edu

**Received** March 06, 2014; **Accepted** October 14, 2014; **Published** February 05, 2015

**Citation:** Rastinehad AR, Fakhoury M, Salami SS, Yaskiv O, Rofeim O, et al. (2015) Intraductal Carcinoma of the Prostate Diagnosed by Multi-Parametric Prostate Magnetic Resonance Imaging (MRI) and MRI/Ultrasound Fusion-Guided Biopsy. Biomedical Data Mining 3: 106. doi: 10.4172/2090-4924.1000106

(Table 1). The peripheral zone was diffusely heterogeneous with two focal suspicious lesions. The first lesion in the right mid gland measured 7×6×9 mm and was triple positive i.e. low signal and focal on T2; low signal with an Apparent Diffusion Coefficient (ADC) value of $794\times10^{-6}$ $mm^2s^{-1}$on Diffusion-Weighted Imaging (DWI); and on Dynamic Contrast Enhancement (DCE), showed avid enhancement with a type 3 curve. The second lesion in the left mid gland peripheral zone was also triple positive with focal low T2 signal; ADC value of $794\times10^{-6}$ $mm^2s^{-1}$; and a type 3 enhancement curve. The b-2000 DWI had diffuse high signal throughout the peripheral zone. There was no evidence of extraprostatic extension (EPE).

The patient underwent MRI/Transrectal Ultrasound (TRUS) Fusion-Guided prostate biopsy (UroNav, Philips Healthcare, Gainesville FL, USA®) of the two suspicious lesions. A standard 12-core TRUS-guided biopsy was then performed. No hypoechoic area suspicious for cancer was identified on TRUS. MRI/TRUS fusion-guided prostate biopsy of the two suspicious lesions detected IDC-P, the largest with a diameter of 10 mm. The first diagnostic biopsy performed showed extensive IDC-P component, present in 16 out of 17 biopsy cores. A single focus of Gleason Score 3+3 adenocarcinoma was identified in one core (1 mm). Pathological diagnosis in this case was challenging because the micropapillary and tufting growth pattern of IDC-P are difficult to differentiate from HGPIN, and therefore require additional diagnostic criteria to confirm the diagnosis. These include nuclear pleomorphism and immunohistochemical staining highlighting basal cells, such as p63, and high molecular weight cytokeratin (HMWCK). Positive staining for the above markers supports the intraductal nature of the lesion. Additionally, alpha-methylacyl-CoA racemase (AMACR or P504S), a marker preferentially expressed in CaP also stained positive.

The patient underwent radical prostatectomy and bilateral pelvic lymph node dissection. Histological examination of the prostate showed a predominantly micropapillary/tufting growth pattern with rare ducts showing loose cribriform morphology. The presence of marked nuclear pleomorphism, non-focal comedonecrosis confirmed the diagnosis of IDC-P. Additionally, conventional/acinar Gleason Score 3+4 invasive adenocarcinoma of the prostate were identified. Intraductal and invasive components of the carcinoma were confined to the prostate gland, rendering a pathological stage pT2 (Figure 2a and b). A total of 3 pelvic lymph nodes removed were negative for malignancy.

## Discussion

Several studies have demonstrated that IDC-P is an aggressive

| | sag t2 | ax vibe | cor t2 | axial t2 | dwi 5 b-values | dwi b-2000 | dce | whole pelv |
|---|---|---|---|---|---|---|---|---|
| # slices | 30 | 30 | 30 | 30 | 30 | 30 | 30 | 88 |
| sithk | 3.0mm | 3.0mm | 3.0mm | 3.0mm | 3.0mm | 3.0mm | 3.0mm | 3.0mm |
| gap | 0 | 0 | 0 | 0 | 0 | 0 | 0 | 20% |
| TR | 4150ms | 3.63ms | 4150ms | 4000ms | 12,600ms | 12,600ms | 3.00ms | 3.92ms |
| TE | 121ms | 1.74ms | 121ms | 120ms | 96ms | 96ms | 0.94ms | 1.39ms |
| FOV | 200mm | 272mm | 200mm | 140mm | 260mm | 260mm | 250mm | 380mm |
| pFOV | 100% | 93.80% | 100% | 100% | 71.6% | 71.6% | 100% | 81.3% |
| AVG | 2 | 1 | 2 | 2 | 2 | 2 | 1 | 1 |
| CONCAT | 2 | 1 | 2 | 2 | 1 | 1 | 1 | 1 |
| DIST CORR | On | On | On | On | On | On | On | On |
| prescan normalize | On | On | On | B1 filter | On | On | On | On |
| pOS | 50% | 50% | 50% | 75% | 50% | 50% | 50% | 0% |
| Phenc | H to F | Rt to Lt | Rt to Lt | Rt to Lt | Rt to Lt | Rt to Lt | Rt to Lt | Rt to Lt |
| flip angle | 150 | 9 | 150 | 132 | | | 12 | 10 |
| fat suppr | None | None | None | None | SPAIR | SPAIR | None | Q-fat sat |
| base res. | 384 | 320 | 384 | 384 | 162 | 162 | 128 | 320 |
| phresol | 95% | 75% | 80% | 80% | 70% | 70% | 100% | 70% |
| ph partial fourler | Off | Off | Off | Off | 6/8 | 6/8 | 7/8 | Off |
| PAT MODE | GRAPPA | GRAPPA | GRAPPA | GRAPPA | GRAPPA | GRAPPA | GRAPPA | GRAPPA |
| ACCEL FACTOR | 2 | 2 | 2 | 2 | 2 | 2 | 2 | 2 |
| Multi-slice mode | Interleave | Sequential | Interleave | Interleave | Interleave | Interleave | Sequential | Sequential |
| posit mode | Isocenter | Isocenter | Isocenter | Isocenter | Isocenter | Isocenter | Isocenter | Isocenter |
| plane | sagittal | axial | coronal | axial | axial | axial | axial | axial |
| Direct | rt to lt | ft to head | A to P | ft to head | ft to head | ft to head | ft to head | ft to head |
| Turbo Factor | 23 | | 23 | 20 | | | | |
| Echo Trains | 121ms | | 11 | 14 | | | | |
| Allowed Delay | 60s | 60s | 60s | 60s | | | 60s | 60s |
| BWTH | 224Hz/Px | 870Hz/Px | 224Hz/Px | 233Hz/Px | 1470Hz/Px | 1470Hz/Px | 1000Hz/Px | 400Hz/Px |
| si OS | | 33.30% | | | | | 33.30% | 9.10% |
| b-values | | | | | 0, 50, 500, 1000, 1500s/mm | 0, 2000s/mm | | |
| EPI factor | | | | | 81 | 81 | | |
| Diff Direct | | | | | 3 | 3 | | |
| Diff Mode | | | | | 3-scan trace | 3-scan trace | | |
| Elliptical scanning | Off | Off | Off | Off | Off | Off | On | Off |
| Slice partial fourler | | | | | | | | 65% |

**Table 1:** MRI Parameters.

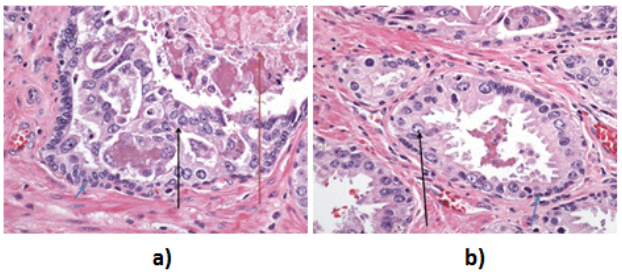


**Figure 2:** 2a) Intraductal carcinoma of the prostate, showing pre-existing prostatic dust, lined by basal cells (blue arrow) and expended by highly pleomorphic cells (black arrow) forming loose cribriform structures. Central comedonecrosis is also present (red arrow). 2b). Intraductal carcinoma of the prostate with preserved basal cells layer (blue arrow) and intraluminal highly pleomorphic cells (black arrow) with tufted architecture.

disease with poor prognosis [7]. Since IDC-P rarely presents as an isolated finding, a diagnosis of IDC-P on prostate biopsy warrants at least immediate repeat biopsy and preferably definitive surgical therapy [4]. The pathological findings in our case, showed extensive IDC-P as well as a focus of invasive carcinoma, prompting definitive surgical intervention. The growing body of literature confirms the importance of reporting IDC-P in biopsy and RP specimens since it is generally associated with an overall poor prognosis. Majority of cases of IDC-P show concomitant high grade (Gleason pattern 4 or 5) and high volume invasive adenocarcinoma. IDC-P associated with low grade (Gleason pattern 3 or less) invasive carcinoma are rare [7].

MP-MRI has been reported to show a predilection for diagnosing high grade CaP, hence IDC-P can be challenging to diagnose when associated with low grade CaP. IDC-P can mimic low grade CaP on T2-weighted MRI, with intermediate to low signal intensity as reported by Schieda et al. [8]. These findings are similar to those observed in our case, in which we presented bilateral low signal (SI 0.39) heterogeneous lesions within the gland on T2-weighted axial image. The ADC map demonstrated restricted areas within the peripheral zone while the DCE showed bilateral enhancement (Figure 1).

Histological features of IDC-P include proliferation of malignant cells within the native prostatic acini and ducts with at least partial preservation of their basal layer.7 McNeal et al. concluded that IDC-P has precise histological criteria with unique biological and clinical significance. The main architectural patterns of growth include solid; dense cribriform (>50% cellularity of the lumen); trabecular/micropapillary; and loose cribriform morphology. Neoplastic cells in IDC-P also show significant nuclear pleomorphism (nuclear enlargement up to 6 times that of adjacent non-neoplastic nuclei). Although, comedonecrosis is an important diagnostic feature of IDC-P, it may not always be present [9].

Cohen et al. have introduced a set of five major criteria for diagnosing IDC-P [10] and include 1) large-caliber glands that are more than twice the diameter of normal peripheral zone gland structures; 2) preserved basal cell layer identified with basal cell markers (34βE12, p63) [11,12]; 3) glands filled with cytological malignant cells (in contrast to those of HG-PIN); 4) the cells always span the gland lumen; and 5) central comedonecrosis. The first 4 major criteria listed are always present in IDC-P. Although central comedonecrosis is not always present, it is a common finding in IDC-P and it is never a feature of HG-PIN. The case presented above met all five of the Cohen criteria. Although comedonecrosis was not identified on prostate biopsy, it was present on subsequent RP specimen.

At the molecular level, evidence supports the distinction of IDC-P amongst its counterparts, through the loss of heterozygosity (LOH) for 12 polymorphic microsatellite markers, known to be frequently lost in CaP. A distinction was made between LOH amounts in HG-PIN, IDC-P, and invasive carcinoma. Study quantifications showed that LOH was absent in Gleason grade 3 cancers, present in 29% of Gleason grade 4 cancers, and commonly found in 60% of IDC-P cases [9].

Clinically, IDC-P is associated with relatively decreased progression free survival [9,12,13] IDC-P found in prostate biopsies is not common, however when it is identified, involvement with high grade and high volume CaP is very likely. Poor prognostic factors such as EPE and SVI were identified in 67% and 44% of patients respectively [3]. Interestingly, Cohen et al. and associates reported that serum PSA levels correlate with tumor volume only when IDC-P was not present in biopsy. These findings suggest that prostate biopsy identified IDC-P counteracts normal and predictive parameters, including PSA and Gleason score. Of note, no nomogram takes into account the presence of IDC-P as masking a high grade or high volume tumor with low PSA. Therefore, IDC-P in biopsies should be reported even when it is associated with high-grade cancer as it may provide prognostic value in management.

## Conclusion

IDC-P is a distinct and aggressive clinic pathologic entity. It is critical to recognize and report IDC-P in prostate specimens in order to improve patient selection for management. IDC-P is strongly associated with aggressive CaP with a high Gleason grade and large tumor volume requiring immediate intervention. We report on a patient with IDC-P identified for the first time by multi-parametric MRI imaging.

### References

1. Rhamy RK, Buchanan RD, Spalding MJ (1973) Intraductal carcinoma of the prostate gland. J Urol 109: 457-460.
2. McNeal JE, Yemoto CE (1996) Spread of adenocarcinoma within prostatic ducts and acini. Morphologic and clinical correlations. Am J Surg Pathol 20: 802-814.
3. Watts K, Li J, Magi-Galluzzi C, Zhou M (2013) Incidence and clinicopathological characteristics of intraductal carcinoma detected in prostate biopsies: a prospective cohort study. Histopathology 63: 574-579.
4. Guo CC, Epstein JI (2006) Intraductal carcinoma of the prostate on needle biopsy: Histologic features and clinical significance. Mod Pathol 19: 1528-1535.
5. Cohen RJ CW, Edgar SC (1998) Prediction of pathological stage and clinical outcome in prostate cancer: an improved pre-operative model incorporating biopsy-determined intraductal carcinoma 81: 413.
6. Robinson B, Magi-Galluzzi C, Zhou M (2012) Intraductal carcinoma of the prostate. Arch Pathol Lab Med 136: 418-425.
7. Cohen RJ, McNeal JE, Baillie T (2000) Patterns of differentiation and proliferation in intraductal carcinoma of the prostate: significance for cancer progression. Prostate 43: 11-19.
8. Schieda N, Coffey, N, Gulavita, P, Al-Dandan, O and Shabana, W, et al. (2014) Prostatic ductal adenocarcinoma: an aggressive tumour variant unrecognized on T2 weighted magnetic resonance imaging (MRI). European Radiology: 330-014-3150-9.
9. Dawkins HJ SL, Turbett GR, Thompson CA, Redmond SL, McNeal JE, , et al. (2000) Distinction between intraductal carcinoma of the prostate (IDC-P), high-grade dysplasia (PIN), and invasive prostatic adenocarcinoma, using molecular markers of cancer progression. Prostate 44: 265-70.

10. Cohen RJ WT, Bonkhoff H, Rubin MA (2007) A proposal on the identification, histologic reporting, and implications of intraductal prostatic carcinoma. Arch Pathol Lab Med 131: 1103-1109.

11. Rubin MA, de La Taille A, Bagiella E, Olsson CA, O'Toole KM (1998) Cribriform carcinoma of the prostate and cribriform prostatic intraepithelial neoplasia: incidence and clinical implications. Am J Surg Pathol 22: 840-848.

12. Wilcox G, Soh S, Chakraborty S, Scardino PT, Wheeler TM (1998) Patterns of high-grade prostatic intraepithelial neoplasia associated with clinically aggressive prostate cancer. Hum Pathol 29: 1119-1123.

13. Shah RB, Magi-Galluzzi C, Han B, Zhou M (2010) Atypical cribriform lesions of the prostate: relationship to prostatic carcinoma and implication for diagnosis in prostate biopsies. Am J Surg Pathol 34: 470-477.